

# cmSalGAN: RGB-D Salient Object Detection with Cross-View Generative Adversarial Networks

Bo Jiang, Zitai Zhou, Xiao Wang, Jin Tang and Bin Luo

**Abstract**—Image salient object detection (SOD) is an active research topic in computer vision and multimedia area. Fusing complementary information of RGB and depth has been demonstrated to be effective for image salient object detection which is known as RGB-D salient object detection problem. The main challenge for RGB-D salient object detection is how to exploit the salient cues of both intra-modality (RGB, depth) and cross-modality simultaneously which is known as cross-modality detection problem. In this paper, we tackle this challenge by designing a novel cross-modality Saliency Generative Adversarial Network (*cmSalGAN*). *cmSalGAN* aims to learn an optimal view-invariant and consistent pixel-level representation for RGB and depth images via a novel adversarial learning framework, which thus incorporates both information of intra-view and correlation information of cross-view images simultaneously for RGB-D saliency detection problem. To further improve the detection results, the attention mechanism and edge detection module are also incorporated into *cmSalGAN*. The entire *cmSalGAN* can be trained in an end-to-end manner by using the standard deep neural network framework. Experimental results show that *cmSalGAN* achieves the new state-of-the-art RGB-D saliency detection performance on several benchmark datasets.

**Index Terms**—RGB-D Saliency Detection, Generative Adversarial Learning, Multi-view Learning

## I. INTRODUCTION

As an important research topic in computer vision and multimedia area, salient object detection (SOD) has attracted more and more attention in recent years. It aims at highlighting salient object regions from the given image and has been widely used in object-level applications in different fields, such as image understanding, object detection, and tracking. The main issues for the SOD task are twofold, i.e., 1) pixel-level representation and 2) saliency prediction/estimation. In the early years, many traditional methods have been proposed for saliency detection by exploiting some low-level feature representations, such as color, HOG, etc. In recent years, with the

This work is supported in part by Major Project for New Generation of AI under Grant (No. 2018AAA0100400); NSFC Key Projects of International (Regional) Cooperation and Exchanges under Grant (61860206004); Open fund for Discipline Construction, Institute of Physical Science and Information Technology, Anhui University

Bo Jiang is with Key Laboratory of Intelligent Computing and Signal Processing of Ministry of Education, School of Computer Science and Technology, Anhui University Institute of Physical Science and Information Technology, Anhui University

Zitai Zhou, Xiao Wang and Bin Luo are with Key Laboratory of Intelligent Computing and Signal Processing of Ministry of Education, School of Computer Science and Technology, Anhui University, Hefei 230601, China.

Jin Tang is with Anhui Provincial Key Laboratory of Multimodal Cognitive Computation, School of Computer Science and Technology, Anhui University, 230601, China

E-mail: {jiangbo, tj, luobin}@ahu.edu.cn, zicair@sina.com, wangxiaocvpr@foxmail.com.

Corresponding author: Xiao Wang

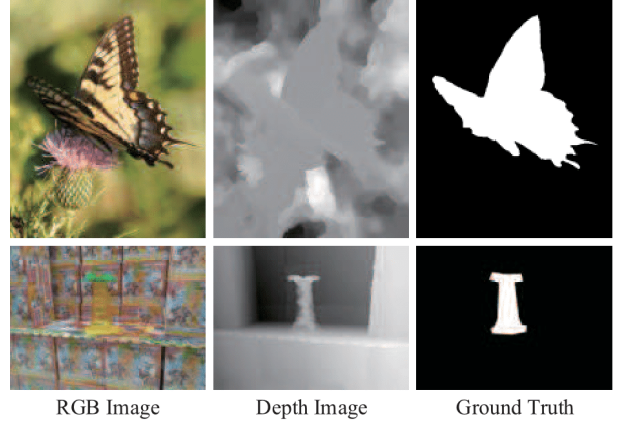


Fig. 1. The illustration of RGB-D saliency detection. The RGB and Depth information can complementary to each other.

development of deep learning-based representation methods, salient object detection has been significantly improved via CNN based pixel-level representation. However, although the salient object detection has made great progress in recent years [1], [2], [3], [4], [5], [6], [7], [8], [9], [10], [11], [12], [13], [14], [15], [16], it is still a challenging problem mainly due to the complicated background and different lighting conditions in the images.

Recently, many works attempt to utilize more modalities to boost the performance of SOD results. One popular way is to integrate the depth information into RGB saliency detection, which is known as RGB-D saliency detection problem. The key idea of RGB-D saliency detection problem is to exploit the complementary information from given modalities for better saliency detection. Since the RGB image contains rich color and texture information while the depth image contains rich depth and contour information. Therefore, how to fuse these modalities in an adaptive and complementary manner is the main challenge of this task. As shown in Figure 1, the ‘butterfly’ object in RGB image is appeared better than that in the depth image, while the salient object in depth image shows better quality in the second row of Figure 1. Therefore, how to fuse these modalities (RGB, depth) adaptively is the key issue to the success of RGB-D salient object detection.

Most of previous works handle the multi-modal fusion problem by *either* serializing the RGB-D channels directly for data representation [17], [18], [19], [20], [21] *or* processing the representation of each modality independently and then combining them together for the final multi-modal representation [7], [22], [23], [24], [25], [26]. Although these strategies

can obtain encouraging results, they are still difficult to fully explore cross-modal complementarity.

In this paper, we propose to address this issue by adopting a generative adversarial learning framework. We develop a novel cross-modality Saliency Generative Adversarial Network (*cmSalGAN*) for RGB-D salient object detection. Overall, *cmSalGAN* aims to learn an optimal modality-invariant and thus can fuse pixel-level representation of RGB and depth images together via a novel adversarial learning framework, which thus incorporates both information of intra-modality and correlation information of cross-modality images simultaneously for the RGB-D saliency detection problem. Specifically speaking, we use two encoder-decoder networks to extract the pixel-level features of RGB and depth images, respectively. We design a novel cross-modality adversarial learning mechanism to boost the representation learning of different modalities, which can achieve the purpose of information fusion. To further improve the detection results, the attention mechanism and edge detection module are also incorporated into *cmSalGAN*. The entire *cmSalGAN* can be trained in an end-to-end manner by using both saliency prediction cross-entropy loss and cross-modality adversarial learning loss.

Note that, generative adversarial networks (GANs) have been designed for image saliency detection tasks [27], [7], [26] and they focus on adversarial learning between saliency prediction and ground-truth salient object. In contrast to previous works, *cmSalGAN* aims to conduct adversarial learning between different modality representations. That is, in *cmSalGAN* the generator and discriminator beat each other as a minimax game to learn discriminative common representation of heterogeneous multi-modality data for the final saliency prediction.

Overall, the main contributions of this paper are summarized as the following three aspects:

- We propose to tackle the problem of cross-modality RGB-D image representation for saliency estimation by exploiting the generative adversarial representation learning. To the best of our knowledge, it is the first work to conduct multi-modality adversarial learning for RGB-D image representation.
- A loss function is designed for cross-modality generative adversarial network (*cmSalGAN*) training to learn a discriminative common presentation for each pixel of RGB and depth images.
- Comprehensive experiments on several widely used RGB-D benchmark datasets validate the effectiveness of the proposed *cmSalGAN* approach. It is also worthy to note that *cmSalGAN* achieves the new state-of-the-art performance on these benchmarks.

The remainder of this paper is organized as follows. In section II, we briefly review some related works on RGB-D saliency detection and Generative Adversarial Networks (GANs). We present the detail of *cmSalGAN* in section III. In section IV, we implement *cmSalGAN* on several benchmarks to demonstrate the effectiveness of the proposed model.

## II. RELATED WORK

In this work, we briefly review the related papers on RGB-D saliency detection and generative adversarial networks.

### A. RGB-D saliency detection

Most of previous works focus on detect saliency objects on the RGB images, for example, Peng *et al.* [13] propose an approach to extract the salient objects in videos automatically. Specifically, they utilize the weighted multiple manifold ranking algorithm to identify object-like regions in each frame. Then, they compute motion cues to estimate the motion saliency and localization prior and finally estimate the superpixel-level object labelling across all frames with a new energy function. Wang *et al.* [2] propose a learning criterion requires the output of the model to be close to the original output. They also propose a hierarchical attribution fusion scheme to enhance the smooth the optimized saliency masks. Koteswar *et al.* [1] adopt the co-saliency detection technique to help exploit the inter-image information, then they perform single-image segmentation on each individual image.

Recently, many works have been proposed for the RGB-D saliency detection problem. The core aspect of these works is how to exploit the salient cues of both inter-modality and intra-modality for the final saliency prediction.

One kind of popular way is to first serialize the RGB-D channels directly for image representation and then conduct saliency prediction. For example, Chen *et al.* [17] propose a PCA network for RGB-D saliency detection which uses a novel complementarity-aware fusion module to deal with the complementarity of two modal information. In work [18], the authors propose a multi-modal fusion network with Multi-scale Multi-path and Cross-modal Interactions (MMCI) network for RGB-D saliency detection. The method aims to use a multi-scale multi-path manner to diversify the contributions of each modality by using a cross-modal interaction. Zhao *et al.* [19] propose a network named Contrast Prior and Fluid Pyramid integration (CPFP) for RGB-D saliency detection which integrates multi-scale cross-modal features by using a pyramid integration model. Chen *et al.* [20] recently propose Three-stream Attention-aware Network (TANet) for RGB-D saliency detection by using a novel triplet-stream multi-modal fusion architecture to extract cross-modal complementary features. Piao *et al.* [21] fuse the cross-modal features and then apply a recurrent attention module to boost the performance.

Another way to handle the multi-modal fusion problem is first processing the representation of each modality independently and then combining them together for the final multi-modal representation. For example, In CTMF [22], it first uses a two-stream architecture to exploit the multi-modal features for RGB and depth images respectively. Then, it aims to merge the representation of the two views to obtain the final saliency maps by using a multi-view CNN fusion model. In work [23], it first extracts handcrafted RGB and depth features in a two-stream network and then fuse them together for RGB-D saliency detection. Wang *et al.* [24] recently propose to employ the U-Net [28] framework to learn a switch map to estimate the weights for fusing RGB

and depth saliency maps together. In addition, inspired by salGAN [27], Wang *et al.* [7] adopt Generative adversarial networks (GANs) for RGB-D saliency detection. They first use MSE and adversarial loss function to extract salient cues for RGB and depth modality, respectively. Then, they employ a reinforcement learning architecture to adaptively fuse these cues together for final saliency prediction. Fan *et al.* [25] propose a depth depurator unit (DDU) to filter out the low-quality depth map and then fuse the cross-modal feature for learning. Liu *et al.* [26] utilize double-stream encoder-decoder network to extract the cross-modal feature and then propose a gated fusion module and employ adversarial learning for RGB-D saliency detection.

Different from previous related works [27], [7], [26], the proposed *cmSalGAN* aims to conduct adversarial learning between different modality representations and to learn a kind of discriminative common representation for both RGB and depth data for saliency prediction.

### B. Generative adversarial networks

Generative adversarial networks (GANs) [29] was originally proposed by Goodfellow *et al.* and have received increasing attention in the fields of machine learning and computer vision fields. Recently, GANs have been exploited for cross-modality visual data representation [30], [31], [32], [33], [34], [35], [36]. For example, Dai *et al.* [31] propose a *cmGAN* network for cross-modality Re-ID task which uses GANs to learn feature representation from different modalities. Lekic *et al.* [32] employs GANs to fuse the radar sensor measurements with the camera images. Gammulle *et al.* [33] apply GANs for fine-grained human action segmentation. Li *et al.* [37] employ GANs to further enhance the retrieval accuracy. Similarly, Zhang *et al.* [38] propose SCH-GAN for semi-supervised cross-modal hashing representation. Dou *et al.* [39] design a cross-modal biomedical image segmentation network via an adversarial learning. Wang *et al.* [40] use GANs to seek an common subspace for cross-modal retrieval. Similarly, Peng *et al.* [41] use GANs to exploit the cross-modal common representations. Ma *et al.* [42] adopt GANs to fuse the information of visible and infrared images. Zhao *et al.* [43] propose a color-depth conditional GAN to concurrently resolve the problem of depth super-resolution and color super-resolution in 3D videos.

Recently, some works also employ GANs for saliency detection tasks. This is because the *pixel-level* measure of saliency results, such as binary cross-entropy loss, can be designed for per-pixel category prediction [44]. However, this pixel-level model generally penalizes the false prediction on every pixel which thus lacks of explicitly modeling the correlation among adjacent pixels and may lead to local inconsistency and semantic inconsistency in the global saliency map prediction. Therefore, some researchers attempt to introduce some *high-level* evaluation criteria, such as adversarial network, to handle these issues. For example, previous works proposed in [27], [45], [46] and [7] all adopt adversarial learning mechanism and achieve better results on RGB or RGB-D related tasks. The adversarial learning mechanism judges whether a given saliency result is real or fake by the joint configuration of many

label variables, and thus can enforce high-level consistency. Specifically, Fernando *et al.* [47] apply GANs for human saliency estimation to jointly model the contextual semantic and relations in different tasks. Pan *et al.* [27] propose Saliency GAN (SalGAN) for saliency prediction task which is trained with MSE and adversarial loss functions. SalGAN360 [48] further extends this framework for the 360° image-based saliency prediction. Wang *et al.* [7] jointly use MSE and adversarial loss function to predict the results of two modalities and then use reinforcement learning to learn the weighted value of the two results. Liu *et al.* [26] propose a gated fusion module for adversarial learning in which the purpose of the discriminator is to learn the gated fusion weights for RGB-D feature extraction.

Previous works [27], [7], [26] focus on adversarial learning between saliency prediction and ground-truth salient object in the later stage. Different from previous adversarial learning based saliency estimation methods, we tackle the problem of cross-modality RGB-D image representation for saliency estimation by exploiting the generative adversarial representation learning. Specifically, *cmSalGAN* aims to conduct adversarial learning between different modality representations and to make the feature of the two modalities complement each other more effectively. To our best knowledge, it is the first work to conduct multi-modality adversarial learning for RGB-D image representation and saliency detection problem, although multi-modality adversarial learning has been studied in other tasks, as summarized in before.

## III. THE PROPOSED METHOD

In this section, we describe the detail of our *cmSalGAN* network. Figure 2 shows the overall of the proposed *cmSalGAN* network which mainly consists of the following four components:

- **Two-stream Generator:** In this paper, we adopt a two-stream network as the generator to learn the feature representation for RGB and depth images respectively. This generator contains two encoder-decoder networks which share the initial weights and are trained to learn their respective network weight parameters.
- **Adversarial Feature Learning:** Following the framework of generative adversarial learning, we introduce a discriminator, *i.e.* Adversarial Feature Learning (AFL) module, to make the features from the two branches combat to each other. This module will enhance the consistent constraint of our saliency detection framework from the perspective of feature learning.
- **Edge Detection Module:** Inspired by existing works [49], [50] which adopt additional edge information for fine-grained segmentation, we also utilize the edge features for more accurate saliency detection in our approach.
- **Saliency Prediction:** We use the de-convolutional layer to restore the resolution of two modalities and feed them into the convolutional layer and ReLU layer to learn the parameters for adaptive fusion. Then, we employ a sigmoid activation function to generate the final saliency prediction.

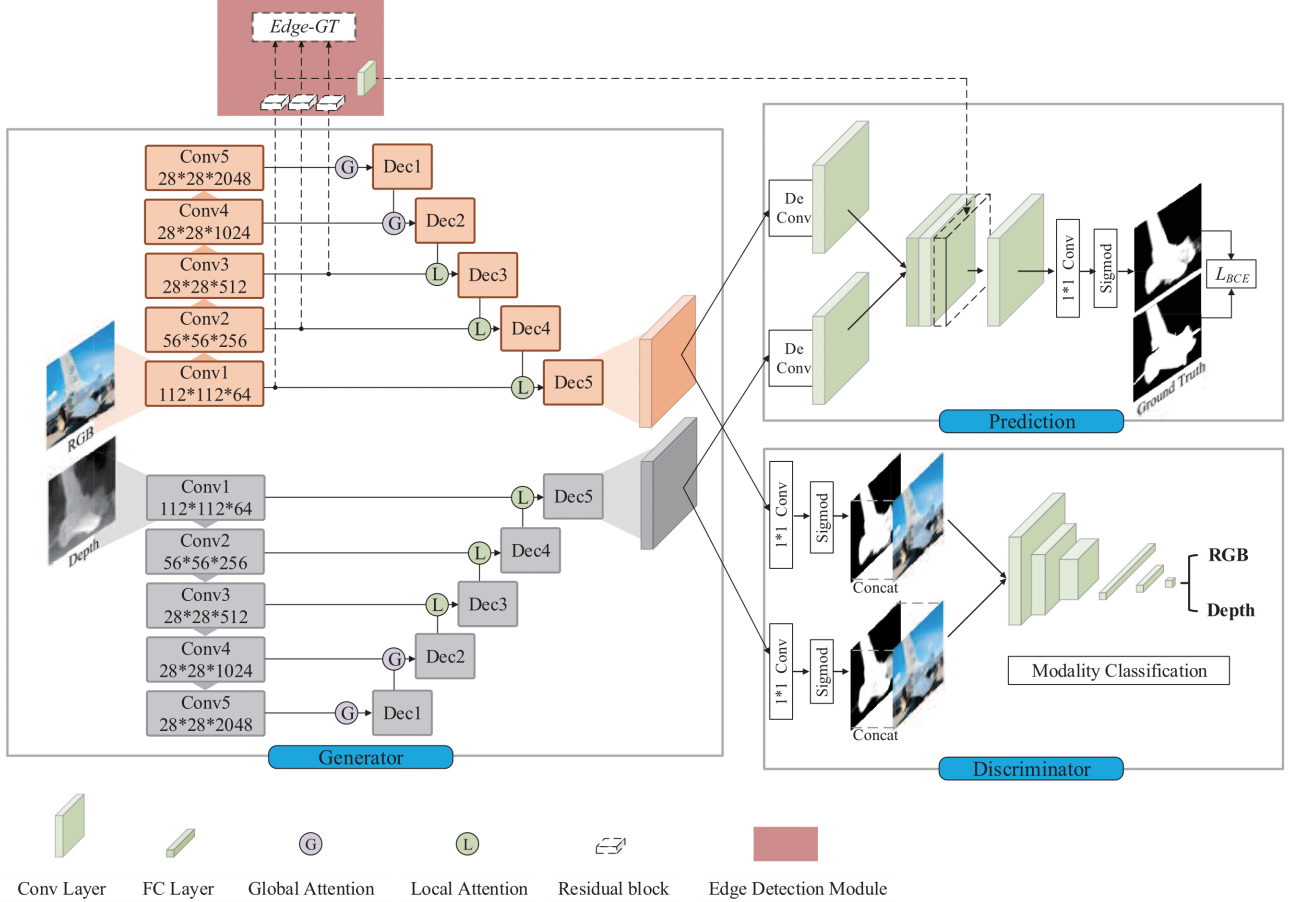


Fig. 2. The illustration of the proposed *cmSalGAN* network for salient object detection. Edge-GT represents the ground truth of the input image when training the edge detection module.

In the following subsections, we will present the details of each component as mentioned above.

#### A. Two-stream Generator

In the feature extraction phase, we utilize a two-stream generator that contains two encode-decoder networks to learn the deep representation of RGB and depth images, respectively. Specifically, the encoder module is a truncated ResNet-50 [51] network (fully connected layers removed) with hole algorithm [52] which can keep the resolutions of feature maps unchanged. The weights of the encoder are initialized with a pre-trained model on the ImageNet dataset [53] for object classification. The input samples are all resized into  $224 \times 224$  and the output feature map  $Enc^i$  from the 1st to 5th convolutional layer ( $Conv_i, i \in \{1, 2, 3, 4, 5\}$ ) has the resolution of 112, 56, 28, 28 and 28 respectively. The decoder contains deconvolutional layers which are used to increase the resolution of the encoded feature map. We use  $Decoder_i, i \in \{1, 2, 3, 4, 5\}$  to denote the corresponding decoder layers. It is worthy to note that the input of depth image is preprocessed into three channels to make it consistent with the RGB branch before feed into the corresponding encoder network.

To obtain better feature representation, we follow the idea of U-Net [28] to fully utilize both low-level and high-level

feature maps in the decoder network by using some skip network connections. This is because different layers contain different information. For example, the lower layers of encoder generally involve rich details while the high-level layers usually contain more semantic information. Therefore, we can obtain a kind of richer decoding feature map  $Dec^i$  by fusing encoder's feature map  $Enc^i$  and decoder's feature map  $Dec^{i-1}$  together. In addition, inspired by work [54], we employ both local and global attention schemes in the decoder network to obtain better feature representation. Specifically, in the global part, we use LSTM [55] in  $Decoder_1$  and  $Decoder_2$  layers to obtain global context information by scanning the input feature maps along both horizontal and vertical directions. In global and local decoder layers, we use an attention mechanism to incorporate multi-scale context information. Given a convolutional feature map  $F \in \mathbb{R}^{W \times H \times C}$  where  $W, H$  and  $C$  denote its width, height and number of channels respectively, we first use a convolutional layer (kernel size is  $1 \times 1$ ) to transform it into a feature map with dimension  $K = W \times H$ . Then, we extract the feature vector  $\mathbf{x}^{w,h} = (x_1^{w,h}, x_2^{w,h}, \dots, x_K^{w,h})$  from each spatial location  $(w, h)$  and the dimension of this vector is  $K$ . Similar to previous work [54], we adopt Softmax function to normalize vector  $\mathbf{x}^{w,h}$  to obtain attention weights  $\alpha^{w,h}$ , the  $\alpha^{w,h}$  can be unfold to  $\alpha^{w,h} = (\alpha_1^{w,h}, \alpha_2^{w,h}, \dots, \alpha_K^{w,h})$ .

TABLE I  
THE DETAILED ARCHITECTURE OF DISCRIMINATOR D.

layer	kernel	activation	out-channel
conv1	$1 \times 1$	ReLU	3
conv2	$3 \times 3$	ReLU	32
max-Pooling	$2 \times 2$	-	32
conv3	$3 \times 3$	ReLU	64
conv4	$3 \times 3$	ReLU	64
max-Pooling	$2 \times 2$	-	64
conv5	$3 \times 3$	ReLU	64
conv6	$3 \times 3$	ReLU	64
max-Pooling	$2 \times 2$	-	64
fc7	-	tanh	100
fc8	-	tanh	2
fc9	-	sigmoid	1

Using the learned  $\alpha^{w,h}$ , we can obtain the attended feature  $F_{attention}^{w,h}$  in each spatial location  $(w, h)$  as [54]

$$F_{attention}^{w,h} = \sum_{i=1}^K \alpha_i^{w,h} f_i \quad (1)$$

where  $f_i \in \mathbb{R}^C$  represents the feature vector at spatial location  $(w, h)$  in  $F$ . Thus we can get the final attention weighted feature  $F_{attention}$ .

### B. Adversarial Feature Learning

In this paper, we employ an adversarial learning to further explore cross-modal complementarity for RGB-D saliency detection task. Generally speaking, we introduce the idea of multi-view learning into the framework of generative adversarial networks [31]. More specifically, we take the output features of RGB and depth modality from the generator as an input of the convolutional (kernel size is  $1 \times 1$ ) and sigmoid layer and generate saliency results from both modalities respectively. Then, we concatenate the predicted saliency results with RGB image and feed them into the discriminator to judge the given results belong to RGB or depth modality. Through the adversarial multi-view learning, we can train the generator to learn a consistent feature representation of the RGB-D image.

The discriminator  $D$  used in our network is a standard convolutional network that contains convolutional layer, ReLU, max-pooling, fully connected layer and sigmoid activation layer. Our discriminator is designed based on [27] and the detailed architecture can be found in Table I. The discriminator is used to judge the given input belongs to the RGB modality or depth modality which will be beneficial for learning a discriminative feature representation. Concretely, after obtaining the feature maps  $Dec_{rgb}^5$  and  $Dec_{depth}^5$  from the two-stream network, we first employ a  $1 \times 1$  convolutional operation on these feature maps and use a sigmoid activation function to obtain the final saliency map  $S_r$  and  $S_d$  whose resolution are all  $112 \times 112 \times 1$ . To make the predicted saliency result consistent with the original image on the resolution, we conduct bilinear interpolation on the saliency map  $S_r$  and  $S_d$  and concatenate them with RGB image to form 4-channel feature maps, respectively. Finally, the feature maps are fed into the adversarial feature learning (AFL) module to achieve

adversarial multi-view learning across different modalities. During the training of our AFL module in which generator and discriminator compete with each other in the form of *mini-max* game to learn the common representation. Similar to [27], the loss function of discriminator can be written as:

$$\mathcal{L}_D = \mathcal{L}(D(I_r, S_r), 1) + \mathcal{L}(D(I_r, S_d), 0) \quad (2)$$

where  $\mathcal{L}$  denotes binary cross entropy loss, and  $D(\cdot, \cdot)$  is the discriminator function used in the adversarial learning procedure.  $I_r$  represents the corresponding original input RGB image. Here we use 1 to denote the target category of RGB sample and 0 for depth sample.

Therefore, the final loss function of the proposed algorithm is formulated as

$$\mathcal{L} = \mathcal{L}_{BCE} + \mathcal{L}(D(I_r, S_r), 0) + \mathcal{L}(D(I_r, S_d), 1) \quad (3)$$

where  $\mathcal{L}_{BCE}$  [56] is defined as

$$\mathcal{L}_{BCE} = \frac{1}{W \times H} \sum_{i=1}^W \sum_{j=1}^H [(1 - S_{ij}) \log(1 - \hat{S}_{ij}) - S_{ij} \log(\hat{S}_{ij})] \quad (4)$$

where  $\hat{S}_{ij}, S_{ij}$  represent the saliency map and corresponding ground truth, respectively.

### C. Edge Detection Module

In order to estimate the final salient object more accurately, inspired by recent work [57], we further introduce an additional edge detection module on the basis of existing network to extract edge features and fuse them into our saliency prediction. Different from previous work [57], we integrate the residual convolutional blocks into the first three convolutional blocks of the encoder to implement feature transformation and edge feature encoding. Since the first three convolutional blocks of the encoder contain more detailed information and they will be more desirable to extract the edge information. Through the first three residual convolutional blocks, we can obtain three kinds of features and all of which have 16 channels. These features are concatenated together and fed into a  $1 \times 1$  convolutional layer to generate the feature map whose dimension is 64. The parameters of the generator are fixed when training the edge detection module and saliency prediction module.

### D. Saliency Prediction

After we obtain the convolutional features of two modalities, we upsample  $Dec_{rgb}^5$  and  $Dec_{depth}^5$  to make them have the same resolution via deconvolutional layers. Then, these two feature maps are concatenated together and fed into a convolutional layer and ReLU layer. Formally, the fused feature map can be transformed into saliency results via a  $1 \times 1$  convolutional operation and sigmoid layer. In this paper, we adopt the commonly used binary cross-entropy (BCE) loss [56] to measure the distance between our saliency prediction and the ground truth saliency map. The loss function  $\mathcal{L}_{BCE}$  is defined as Eq. (4), where  $\hat{S}_{ij}, S_{ij}$  represent the saliency map and corresponding ground truth, respectively.

#### IV. EXPERIMENTS

To evaluate the effectiveness of the proposed *cmSalGAN* approach, we test it on three benchmark datasets. In the following, we first introduce the datasets and evaluation metrics used in our experiments. Then, we present the implementation details of our *cmSalGAN* saliency detection algorithm. Finally, we compare our method with other state-of-the-art RGB-D saliency detection algorithms and further conduct the ablation studies for the proposed *cmSalGAN* model.

##### A. Datasets and Evaluation Metrics

**Datasets:** Three widely used RGB-D saliency detection benchmark datasets are used to evaluate our *cmSalGAN* method, i.e., NJUD [58], NLPR [59] and STEREO [6]. NJUD dataset [58] contains 2003 stereo images that are collected from the Internet, 3D movies and photographs acquired by a stereo camera. Then, the optical flow technique [60] is adopted to recover the depth maps. NLPR dataset [59] consists of 1000 images which are all taken by Kinect under different lighting conditions including both indoors and outdoors. The images in this dataset are selected from 5000 natural images and their depth maps and the saliency regions are annotated by five participants. STEREO dataset [6] consists of 797 stereo images.

For fair comparison, we adopt the same protocol to separate each dataset, as introduced in work [22]. The training subset contains 1400 and 650 samples from NJUD and NLPR dataset respectively. The validation set contains 100 samples from the NJUD and 50 samples from the NLPR dataset. The remaining samples in NJUD and NLPR and all the images in the STEREO dataset are used for testing.

**Evaluation Metrics:** To achieve a comprehensive evaluation of the proposed *cmSalGAN* saliency detection method and other comparison detectors, we adopt four standard evaluation metrics to evaluate the predicted saliency maps, including Precision-Recall (PR) curve, S-measure scores, Mean Absolute Error (MAE) and maximal F-measure. Specifically, Precision-recall curve [61] is one of the most popular evaluation metric for saliency detection. S-measure [62] is a metric which evaluates both region-aware  $S_{region}$  and object-aware  $S_{object}$  structural similarity between saliency output and ground truth map, which can be formulated as:

$$\text{S-measure} = \alpha S_{object} + (1 - \alpha) S_{region} \quad (5)$$

MAE [3] is defined as the average pixel-wise absolute difference between the saliency output and the ground truth map which is defined as

$$MAE = \frac{1}{W \times H} \sum_{x=1}^W \sum_{y=1}^H |S(x, y) - G(x, y)| \quad (6)$$

The F-measure [63] is a balanced mean of average precision and average recall which is calculated as

$$F = \frac{(1 + \beta^2) \times Precision \times Recall}{\beta^2 \times Precision + Recall} \quad (7)$$

where  $\beta^2$  is set as 0.3, as suggested in most previous works [7], [27]. The definition of precision and recall are:

$$Precision = \frac{TP}{TP + FP}; \quad Recall = \frac{TP}{TP + FN} \quad (8)$$

where TP, FP, TN and FN denote the numbers of true positives, false positives, true negatives and false negatives, respectively.

##### B. Implementation Details

Due to the limited images in the RGB-D saliency detection datasets, similar to previous related works [19], [18], [22], [20], [17], we adopt horizontal flip and random crop to augment the training data. In addition, we also add supervision with a smaller weight to each layer of the decoders so that being able to guide the decoder layers to learn better feature representation. The weight ratios of the five layers are set to  $\{0.5, 0.5, 0.5, 0.8, 0.8\}$  respectively. In the *cmSalGAN* framework, the generator and discriminator are alternately trained according to batchsize. When training the discriminator, only the parameters of the discriminator are updated. When the generator is trained, the gradient of the discriminator is reversely transmitted to the generator and update the parameters of the generator. It is also worthy to note that the proposed Adversarial Feature Learning module is only used in the training phase to consistently learn the multi-modal adversarial features. That is, only the two-stream generator and feature fusion module are used in the test phase. Our model is implemented based on PyTorch and all experiments are implemented with a NVIDIA 1080Ti GPU. The Adam [64] optimizer is used for the training and the learning rate and batch size are set to 0.0001 and 4 respectively. We train the network for 180 epochs which cost 91 hours and each image takes 0.88s during the test phase. We fine-tune 10 epochs on the edge detection dataset [57] when adding edge module. Our *cmSalGAN* is an end-to-end network, which has no pre-training stage or other post-processing operations.

##### C. Comparison results

We compare our *cmSalGAN* with ten state-of-the-art deep learning based RGB-D salient object detection models including CTMF [22], PCA [17], MMCI [18], CPFP [19], TANet [20], GAN-RL [7], AF [24], D3Net [25], DMRA-Net [21] and GFNet [26]. Note that CTMF [22], PCA [17], MMCI [18] and TANet [20] adopt VGG16 [66] as backbone while D3Net [25] adopt resnet50 [51], and they all use cross-entropy loss function. GAN-RL [7] adopt VGG16 [66] as backbone and use mean squared and adversarial loss, while GFNet [26] use cross-entropy and adversarial loss. CPFP [19] adopt VGG16 [66] and use cross-entropy and contrast loss. AF [24] adopt VGG16 [66] and use cross-entropy and edge-preserving loss. DMRA-Net [21] adopt VGG19 [66] and use softmax-entropy loss. In addition, we also report some traditional RGB-D salient object detection methods including DES [5], ACSD [58], DCMC [4] and LBE [65]. For comparison method CTMF [22], PCA [17], MMCI [18], TANet [20], ACSD [58], DES [5], LBE [65], GAN-RL [7] and D3Net [25], we directly evaluate the saliency maps of corresponding algorithm provided by

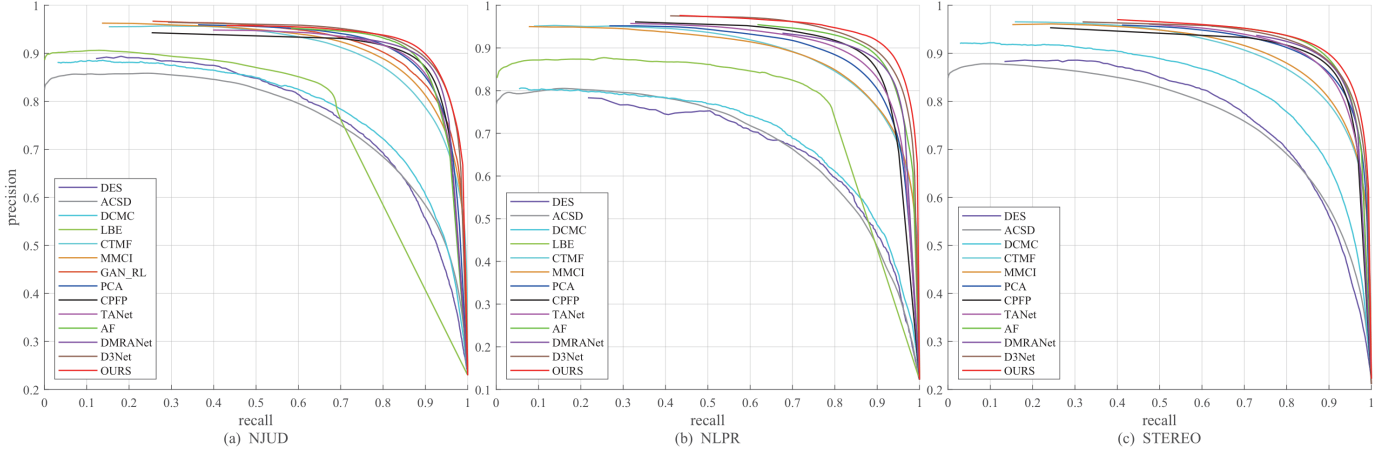


Fig. 3. Visual comparison P-R curves on NJUD, NLPR and STEREO respectively.

TABLE II

COMPARISON OF DIFFERENT METHODS ON NJUD, NLPR AND STEREO DATASETS RESPECTIVELY. THE EVALUATION MEASUREMENTS CONTAIN MAXIMAL F-MEASURE, S-MEASURE AND MAE, RESPECTIVELY. THE TOP 2 DETECTION RESULTS ARE HIGHLIGHTED IN RED AND GREEN, RESPECTIVELY.

Method	NJUD			NLPR			STEREO		
	F-measure	S-measure	MAE	F-measure	S-measure	MAE	F-measure	S-measure	MAE
DES[5]	0.7083	0.6620	0.2896	0.6391	0.5727	0.3164	0.7275	0.6697	0.2821
ACSD[58]	0.7110	0.7018	0.1905	0.6436	0.6987	0.1560	0.7171	0.7138	0.1840
DCMC[4]	0.7220	0.6895	0.1674	0.6556	0.7288	0.1122	0.7586	0.7376	0.1500
LBE[65]	0.7456	0.7003	0.1490	0.7576	0.7769	0.0731	-	-	-
CTMF[22]	0.8441	0.8490	0.0847	0.8255	0.8599	0.0561	0.8385	0.8529	0.0867
GAN-RL [7]	0.8679	0.8681	0.0803	-	-	-	-	-	-
PCA[17]	0.8722	0.8770	0.0591	0.8410	0.8736	0.0437	0.8700	0.8800	0.0606
MMCI[18]	0.8518	0.8581	0.0790	0.8148	0.8557	0.0591	0.8425	0.8559	0.0796
TANet[20]	0.8737	0.8782	0.0605	0.8632	0.8861	0.0410	0.8705	0.8775	0.0591
CPP[19]	0.8767	0.8777	0.0533	0.8675	0.8884	0.0360	0.8738	0.8792	0.0514
AF[24]	0.8819	0.8813	0.0532	0.8851	0.9011	0.0329	0.8907	0.8921	0.0472
DMRANet[21]	0.8857	0.8854	0.0509	0.8792	0.8984	0.0313	0.8857	0.8854	0.0475
D3Net[25]	0.8885	0.8946	0.0509	0.8854	0.9056	0.0341	0.8809	0.8907	0.0541
GFNet[26]	-	0.8851	0.0517	-	0.9075	0.0296	-	0.8806	0.0495
<i>cmSalGAN-Edge</i>	<b>0.8932</b>	<b>0.9000</b>	<b>0.0486</b>	<b>0.9037</b>	<b>0.9173</b>	<b>0.0286</b>	<b>0.8912</b>	<b>0.8978</b>	0.0523
<i>cmSalGAN</i>	<b>0.8965</b>	<b>0.9034</b>	<b>0.0462</b>	<b>0.9070</b>	<b>0.9224</b>	<b>0.0267</b>	<b>0.8938</b>	<b>0.8999</b>	0.0496

the authors. For GFNet [26], we obtain the evaluation result directly from the paper. For the other comparison methods, we run the original codes with default settings provided by the authors. For evaluation measurements, we use the *evaluation tool*<sup>1</sup> provided by Wang *et al.* [67].

Figure 3 shows the comparison results on PR curve. One can note that the proposed *cmSalGAN* achieves the best performance on all three datasets, especially on the NLPR dataset. This suggests the effectiveness of the proposed *cmSalGAN* method. Table II summarizes the comparison results on MAE, maximal F-measure, and S-measure, respectively. Our proposed method generally performs better than other comparison methods on most of the evaluation measurements and datasets. This also fully validates the effectiveness and advantages of the proposed *cmSalGAN* method. More specifically, *cmSalGAN* outperforms GAN-RL [7] and GFNet [26] which also employ adversarial feature learning for RGB-D saliency detection. As discussed before, GAN-RL conducts adversarial learning for RGB and depth modality separately and adaptively fuses

these results as post-processing by reinforcement learning architecture. GFNet construct a gated fusion module for cross-modal feature fusion through adversarial learning. GAN-RL achieves 0.8679 on maximal F-measure on the NJUD dataset while the propose method achieves 0.8965, GFNet achieves 0.8851 on S-measure on the NJUD dataset while the proposed method achieves 0.9034. This obviously demonstrates the advantages of the proposed cross-view adversarial learning. In addition, as shown in the Table II we can see that the variation *cmSalGAN-Edge* (i.e. the framework without Edge module) also achieves the state-of-the-art performance.

Figure 4 shows some qualitative results to better demonstrate the advantages of the proposed saliency detection method. Intuitively, *cmSalGAN* obtains the best saliency detection results compared with other approaches. Specifically, our approach can produce more fine-grained details as highlighted in the salient region as shown in the 1<sup>st</sup> and 2<sup>nd</sup> rows in Figure 4. We can also observe that the depth image in the 7<sup>th</sup> row contains some misleading salience cues that make it difficult to distinguish interferences in depth information. However, our method still works well in such challenging

<sup>1</sup> <https://github.com/wenguangwang/SODsurvey/>

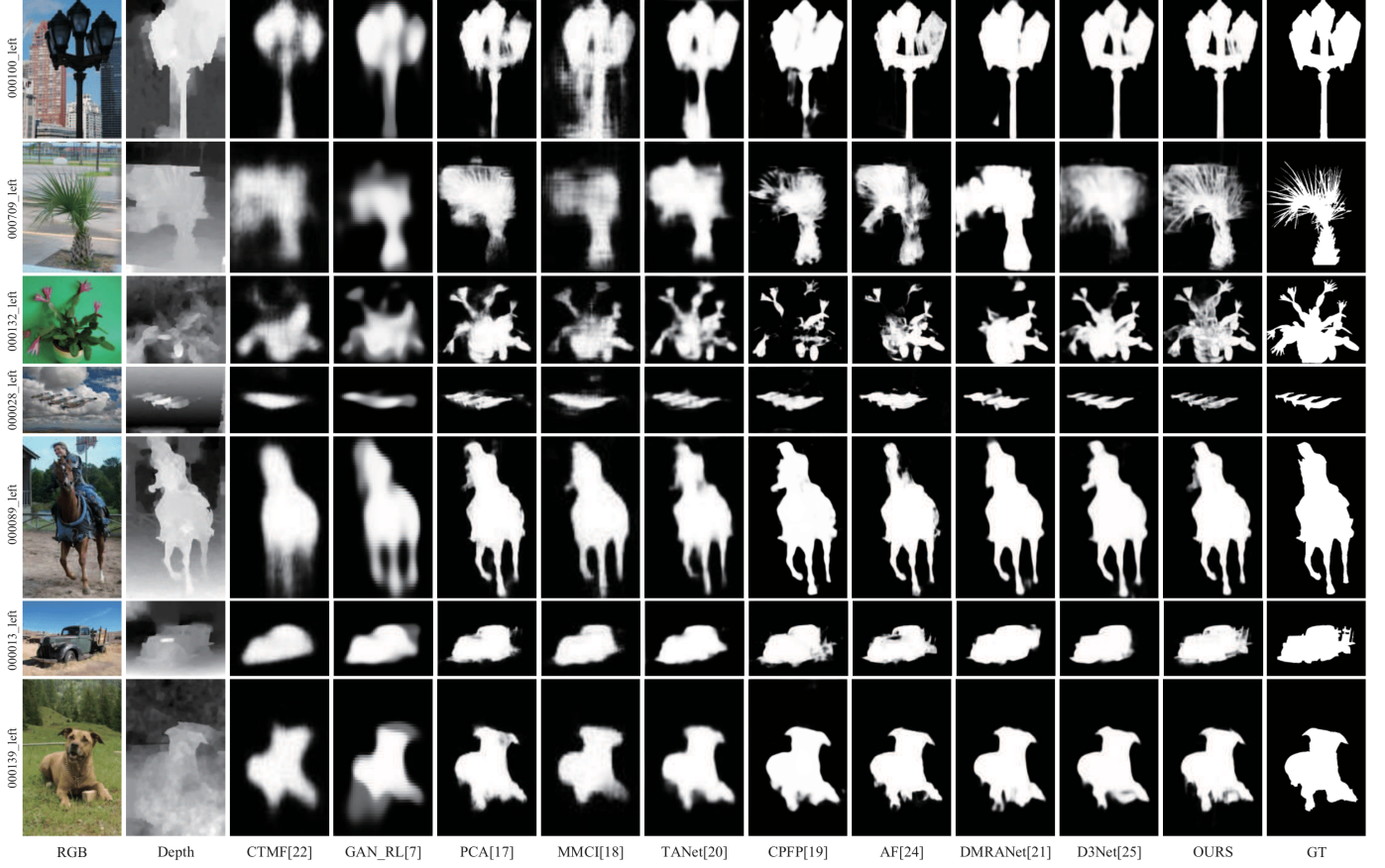


Fig. 4. Qualitative visual comparisons to other state-of-the-art CNNs-based methods and the last column GT represents the ground truth.

TABLE III

THE EVALUATION OF MAXIMAL F-MEASURE, S-MEASURE AND MAE ON NJUD, NLPR AND STEREO RESPECTIVELY.  $G_{Depth}$  AND  $G_{RGB}$  REPRESENT THE DEPTH AND RGB BRANCH OF OUR GENERATOR RESPECTIVELY.  $G_{RGB+Depth}$  REPRESENT FUSE RGB AND DEPTH SIMPLY. '+G' AND '+L' REPRESENT ADD THE GLOBAL AND LOCAL ATTENTION SCHEME.

Method	NJUD			NLPR			STEREO		
	F-measure	S-measure	MAE	F-measure	S-measure	MAE	F-measure	S-measure	MAE
$G_{Depth}$	0.8103	0.8351	0.0948	0.7884	0.8276	0.0739	0.7119	0.7659	0.1289
$G_{Depth} + LG$	0.8239	0.8498	0.0834	0.8308	0.8622	0.0566	0.7283	0.7754	0.1196
$G_{RGB}$	0.8292	0.8496	0.0762	0.8362	0.8685	0.0537	0.8383	0.8554	0.0807
$G_{RGB} + LG$	0.8560	0.8728	0.0610	0.8682	0.8971	0.0362	0.8728	0.8846	0.0597
$G_{RGB+Depth}$	0.8680	0.8811	0.0599	0.8708	0.8959	0.0403	0.8593	0.8757	0.0668
$G_{RGB+Depth} + G$	0.8779	0.8823	0.0672	0.8819	0.9009	0.0428	0.8590	0.8707	0.0774
$G_{RGB+Depth} + L$	0.8736	0.8843	0.0600	0.8775	0.9028	0.0374	0.8578	0.8724	0.0663
$G_{RGB+Depth} + LG$	0.8854	0.8891	0.0527	0.8855	0.9043	0.0322	0.8613	0.8677	0.0626

scenarios. These conclusions can also be drawn from the rest of the images.

#### D. Ablation Studies

In this section, we conduct some ablation studies to better understand the effect of each component in our model. Specifically speaking, we will first check the effect of dual-modality fusion and the effect of global and local attention scheme in the generator. Then, we will discuss the effect of adversarial feature learning module and edge information. Finally, we will discuss the limitations of the proposed RGB-D salient object detection algorithm.

**Effectiveness of dual-modality fusion.** We compare the proposed approach with only one modality used version to

validate the effectiveness of the fusion module for RGB-D saliency detection. As shown in Table III, it is easy to find that the result of fused RGB-D saliency detection is significantly better than only one modality used version on all the three datasets. For example, the results of  $G_{Depth}$  and  $G_{RGB}$  achieve 0.8103 and 0.8292 on maximal F-measure on the NJUD dataset respectively, while the  $G_{RGB+Depth}$  method which fuse RGB and depth features together achieves 0.8680 which is a significant improvement. Similar conclusions can also be drawn from other evaluation metrics and benchmark datasets. These experiments all validated the effectiveness of dual-modality fusion for saliency detection.

**Effectiveness of attention module.** To validate the effectiveness of our used global or local attention modules, we con-

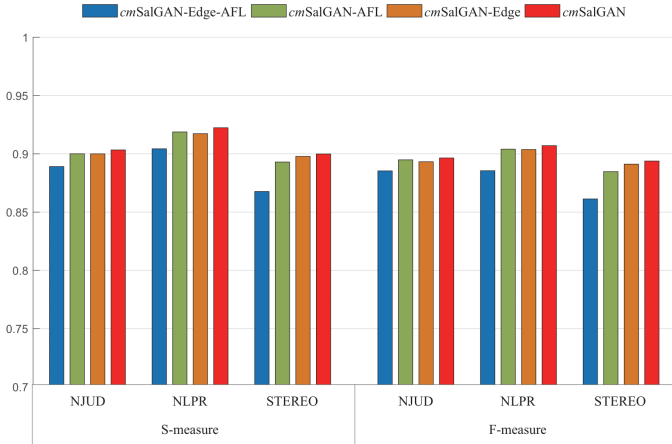


Fig. 5. Comparisons of S-measure and maximal F-measure to evaluate the contribution of AFL module and Edge module. '-Edge' and '-AFL' represent the *cmSalGAN* network without Edge and AFL modules.

duct related analysis in the following subsection. As reported in Table III, all variants of our saliency detection algorithm can boost its performance with attention model on the used three benchmarks. More detail, the maximal F-measure score on the NJUD dataset of  $G_{Depth} + LG$  and  $G_{RGB} + LG$  all increased to 0.8239 and 0.8560. The  $G_{RGB+Depth}$  achieves 0.8680 on maximal F-measure while  $G_{RGB+Depth} + LG$  achieves 0.8854.

**Effectiveness of AFL and Edge components.** To validate the effectiveness of AFL and Edge components in our network, we implement four variations of the model:

- 1) *cmSalGAN*-Edge-AFL that removes Edge and AFL module, only use BCE loss function in the training phase.
- 2) *cmSalGAN*-AFL that removes AFL module.
- 3) *cmSalGAN*-Edge that removes Edge module.
- 4) *cmSalGAN* that adds Edge and AFL module.

As shown in Fig. 5, we can note that: (1) Remove the Edge and AFL module, the saliency detection results dropped in all three benchmark datasets. (2) The overall performance can be improved with the Edge module (i.e. the framework with BCE loss function and Edge module). (3) Add AFL module could improve the performance of our saliency detection network, which validate the effectiveness of the AFL module. We can obtain 0.8932, 0.9037 and 0.8912 on the maximal F-measure on the NJUD, NLPR, and STEREO as shown in Table II. And it achieves the state of the art performance. (4) We introduce an edge detection module in the shallow layer of the encoder which can further improve the performance of our *cmSalGAN* network. This experiment validates the effectiveness of the Edge module. When integrating the edge feature into our model, we can achieve better saliency detection performance. More detail, we can obtain 0.8965, 0.9070, 0.8938 on the maximal F-measure on the NJUD, NLPR and STEREO.

We also conduct a visual comparison of saliency maps generated by these four variants of our model in Figure 6. From both qualitative and quantitative analysis, we can observe that the proposed adversarial feature learning module can significantly improve the deep representation learning for RGB-D saliency detection. And integrate the edge feature

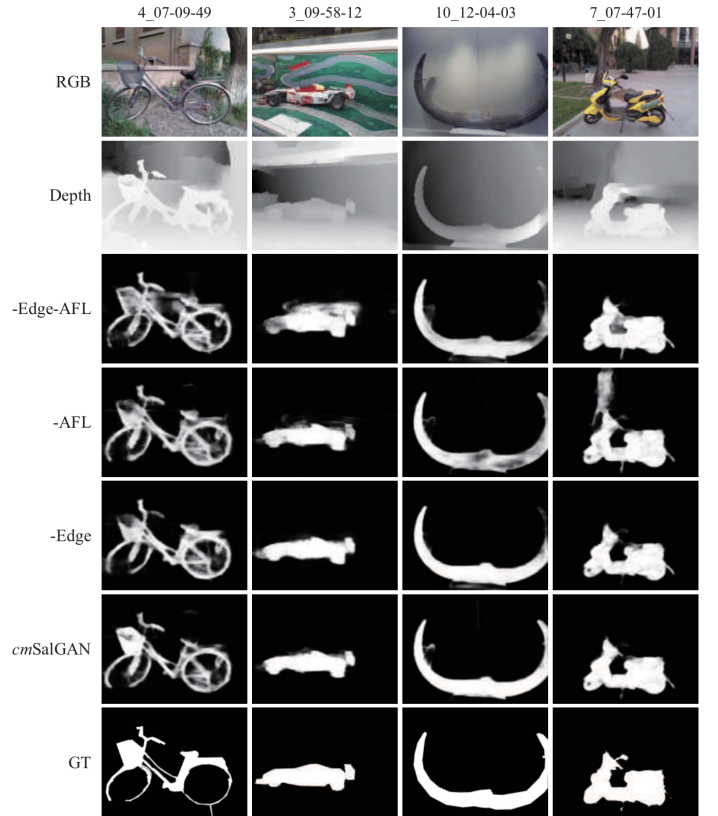


Fig. 6. Visualization of saliency detection results for different variations of the model. '-Edge' and '-AFL' represent the *cmSalGAN* network without Edge and AFL modules.

into our model could further improve the performance of the saliency detection network.

## V. CONCLUSION

In this paper, we design an end-to-end RGB-D salient object detection framework based on generative adversarial feature learning. Our framework utilizes a two-stream generator to learn the feature representations of RGB and depth, respectively. We creatively fuse the features of RGB and depth with a feature embedding module to handle the limitations of single modality. More importantly, we conduct the adversarial feature learning between both RGB and depth modalities to boost their deep representations in the training stage. Our experiments validated the effectiveness of the proposed method on multiple saliency detection benchmarks. Note that, the proposed *cmSalGAN* provides a general framework for RGB-D saliency detection tasks. Our module can be incorporated into many RGB-D algorithms to further improve their final performance.

## REFERENCES

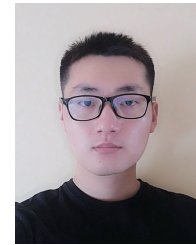
- [1] Koteswar Rao Jerripothula, Jianfei Cai, and Junsong Yuan. Image co-segmentation via saliency co-fusion. *IEEE Transactions on Multimedia*, 18(9):1896–1909, 2016.
- [2] Yulong Wang, Hang Su, Bo Zhang, and Xiaolin Hu. Learning reliable visual saliency for model explanations. *IEEE Transactions on Multimedia*, 2019.
- [3] Federico Perazzi, Philipp Krähenbühl, Yael Pritch, and Alexander Hornung. Saliency filters: Contrast based filtering for salient region detection. In *2012 IEEE conference on computer vision and pattern recognition*, pages 733–740. IEEE, 2012.

- [4] Runmin Cong, Jianjun Lei, Changqing Zhang, Qingming Huang, Xiaochun Cao, and Chunping Hou. Saliency detection for stereoscopic images based on depth confidence analysis and multiple cues fusion. *IEEE Signal Processing Letters*, 23(6):819–823, 2016.
- [5] Yupeng Cheng, Huazhu Fu, Xingxing Wei, Jiangjian Xiao, and Xiaochun Cao. Depth enhanced saliency detection method. In *Proceedings of international conference on internet multimedia computing and service*, pages 23–27, 2014.
- [6] Yuzhen Niu, Yujie Geng, Xueqing Li, and Feng Liu. Leveraging stereopsis for saliency analysis. In *2012 IEEE Conference on Computer Vision and Pattern Recognition*, pages 454–461. IEEE, 2012.
- [7] Xiao Wang, Tao Sun, Rui Yang, Chenglong Li, Bin Luo, and Jin Tang. Quality-aware dual-modal saliency detection via deep reinforcement learning. *Signal Processing: Image Communication*, 75:158–167, 2019.
- [8] Andrea Rosani, Giulia Boato, and Francesco GB De Natale. Eventmask: A game-based framework for event-saliency identification in images. *IEEE Transactions on Multimedia*, 17(8):1359–1371, 2015.
- [9] Ji Hwan Park, Ievgeniia Gutenko, and Arie E Kaufman. Transfer function-guided saliency-aware compression for transmitting volumetric data. *IEEE Transactions on Multimedia*, 2017.
- [10] Youbao Tang and Xiangqian Wu. Salient object detection using cascaded convolutional neural networks and adversarial learning. *IEEE Transactions on Multimedia*, 2019.
- [11] Jin-Gang Yu, Gui-Song Xia, Changxin Gao, and Ashok Samal. A computational model for object-based visual saliency: Spreading attention along gestalt cues. *IEEE Transactions on Multimedia*, 18(2):273–286, 2015.
- [12] Haorun Liang, Ronghua Liang, and Guodao Sun. Looking into saliency model via space-time visualization. *IEEE Transactions on Multimedia*, 18(11):2271–2281, 2016.
- [13] Qinmu Peng and Yiu-ming Cheung. Automatic video object segmentation based on visual and motion saliency. *IEEE Transactions on Multimedia*, 2019.
- [14] Mingzhu Xu, Bing Liu, Ping Fu, Junbao Li, and Yu Hen Hu. Video saliency detection via graph clustering with motion energy and spatiotemporal objectness. *IEEE Transactions on Multimedia*, 2019.
- [15] Yunxiao Li, Shuai Li, Chenglizhao Chen, Hong Qin, and Aimin Hao. Accurate and robust video saliency detection via self-paced diffusion. *IEEE Transactions on Multimedia*, 2019.
- [16] Cheng Deng, Xu Yang, Feiping Nie, and Dapeng Tao. Saliency detection via a multiple self-weighted graph-based manifold ranking. *IEEE Transactions on Multimedia*, 2019.
- [17] Hao Chen and Youfu Li. Progressively complementarity-aware fusion network for rgb-d salient object detection. In *Proceedings of the IEEE Conference on Computer Vision and Pattern Recognition*, pages 3051–3060, 2018.
- [18] Hao Chen, Youfu Li, and Dan Su. Multi-modal fusion network with multi-scale multi-path and cross-modal interactions for rgb-d salient object detection. *Pattern Recognition*, 86:376–385, 2019.
- [19] Jia-Xing Zhao, Yang Cao, Deng-Ping Fan, Ming-Ming Cheng, Xuan-Yi Li, and Le Zhang. Contrast prior and fluid pyramid integration for rgbd salient object detection. In *Proceedings of the IEEE Conference on Computer Vision and Pattern Recognition*, pages 3927–3936, 2019.
- [20] Hao Chen and Youfu Li. Three-stream attention-aware network for rgbd salient object detection. *IEEE Transactions on Image Processing*, 28(6):2825–2835, 2019.
- [21] Yongri Piao, Wei Ji, Jingjing Li, Miao Zhang, and Huchuan Lu. Depth-induced multi-scale recurrent attention network for saliency detection. In *Proceedings of the IEEE International Conference on Computer Vision*, pages 7254–7263, 2019.
- [22] Junwei Han, Hao Chen, Nian Liu, Chenggang Yan, and Xuelong Li. Cnns-based rgbd saliency detection via cross-view transfer and multiview fusion. *IEEE transactions on cybernetics*, 48(11):3171–3183, 2017.
- [23] Riku Shigematsu, David Feng, Shaodi You, and Nick Barnes. Learning rgbd salient object detection using background enclosure, depth contrast, and top-down features. In *Proceedings of the IEEE International Conference on Computer Vision Workshops*, pages 2749–2757, 2017.
- [24] Ningning Wang and Xiaojin Gong. Adaptive fusion for rgbd salient object detection. *IEEE Access*, 7:55277–55284, 2019.
- [25] Deng-Ping Fan, Zheng Lin, Jia-Xing Zhao, Yun Liu, Zhao Zhang, Qibin Hou, Menglong Zhu, and Ming-Ming Cheng. Rethinking rgbd salient object detection: Models, datasets, and large-scale benchmarks. *arXiv preprint arXiv:1907.06781*, 2019.
- [26] Zhengyi Liu, Wei Zhang, and Peng Zhao. A cross-modal adaptive gated fusion generative adversarial network for rgbd salient object detection. *Neurocomputing*, 387:210 – 220, 2020.
- [27] Junting Pan, Cristian Canton Ferrer, Kevin McGuinness, Noel E O’Connor, Jordi Torres, Elisa Sayrol, and Xavier Giro-i Nieto. Salgan: Visual saliency prediction with generative adversarial networks. *arXiv preprint arXiv:1701.01081*, 2017.
- [28] Olaf Ronneberger, Philipp Fischer, and Thomas Brox. U-net: Convolutional networks for biomedical image segmentation. In *International Conference on Medical image computing and computer-assisted intervention*, pages 234–241. Springer, 2015.
- [29] Ian Goodfellow, Jean Pouget-Abadie, Mehdi Mirza, Bing Xu, David Warde-Farley, Sherjil Ozair, Aaron Courville, and Yoshua Bengio. Generative adversarial nets. In *Advances in neural information processing systems*, pages 2672–2680, 2014.
- [30] Konstantinos Bousmalis, Nathan Silberman, David Dohan, Dumitru Erhan, and Dilip Krishnan. Unsupervised pixel-level domain adaptation with generative adversarial networks. In *Proceedings of the IEEE conference on computer vision and pattern recognition*, pages 3722–3731, 2017.
- [31] Pingyang Dai, Rongrong Ji, Haibin Wang, Qiong Wu, and Yuyu Huang. Cross-modality person re-identification with generative adversarial training. In *IJCAI*, volume 1, page 2, 2018.
- [32] Vladimir Lekic and Zdenka Babic. Automotive radar and camera fusion using generative adversarial networks. *Computer Vision and Image Understanding*, 184:1–8, 2019.
- [33] Harshala Gammulle, Tharindu Fernando, Simon Denman, Sridha Sridharan, and Clinton Fookes. Coupled generative adversarial network for continuous fine-grained action segmentation. In *2019 IEEE Winter Conference on Applications of Computer Vision*, pages 200–209. IEEE, 2019.
- [34] Xiaopeng Guo, Rencan Nie, Jinde Cao, Dongming Zhou, Liye Mei, and Kangjian He. Fusegan: Learning to fuse multi-focus image via conditional generative adversarial network. *IEEE Transactions on Multimedia*, 21(8):1982–1996, 2019.
- [35] Biting Yu, Luping Zhou, Lei Wang, Yinghuan Shi, Jurgen Fripp, and Pierrick Bourgeat. Ea-gans: edge-aware generative adversarial networks for cross-modality mr image synthesis. *IEEE transactions on medical imaging*, 38(7):1750–1762, 2019.
- [36] De Xie, Cheng Deng, Chao Li, Xianglong Liu, and Dacheng Tao. Multi-task consistency-preserving adversarial hashing for cross-modal retrieval. *IEEE Transactions on Image Processing*, 29:3626–3637, 2020.
- [37] Chao Li, Cheng Deng, Ning Li, Wei Liu, Xinbo Gao, and Dacheng Tao. Self-supervised adversarial hashing networks for cross-modal retrieval. In *Proceedings of the IEEE conference on computer vision and pattern recognition*, pages 4242–4251, 2018.
- [38] Jian Zhang, Yuxin Peng, and Mingkuan Yuan. Sch-gan: Semi-supervised cross-modal hashing by generative adversarial network. *IEEE transactions on cybernetics*, 50(2):489–502, 2018.
- [39] Qi Dou, Cheng Ouyang, Cheng Chen, Hao Chen, and Pheng-Ann Heng. Unsupervised cross-modality domain adaptation of convnets for biomedical image segmentations with adversarial loss. *arXiv preprint arXiv:1804.10916*, 2018.
- [40] Bokun Wang, Yang Yang, Xing Xu, Alan Hanjalic, and Heng Tao Shen. Adversarial cross-modal retrieval. In *Proceedings of the 25th ACM international conference on Multimedia*, pages 154–162, 2017.
- [41] Yuxin Peng and Jinwei Qi. Cm-gans: Cross-modal generative adversarial networks for common representation learning. *ACM Transactions on Multimedia Computing, Communications, and Applications*, 15(1):1–24, 2019.
- [42] Jiayi Ma, Wei Yu, Pengwei Liang, Chang Li, and Junjun Jiang. Fusion-gan: A generative adversarial network for infrared and visible image fusion. *Information Fusion*, 48:11–26, 2019.
- [43] Lijun Zhao, Huihui Bai, Jie Liang, Bing Zeng, Anhong Wang, and Yao Zhao. Simultaneous color-depth super-resolution with conditional generative adversarial networks. *Pattern Recognition*, 88:356–369, 2019.
- [44] Yawei Luo, Zhedong Zheng, Liang Zheng, Tao Guan, Junqing Yu, and Yi Yang. Macro-micro adversarial network for human parsing. In *Proceedings of the European Conference on Computer Vision*, pages 418–434, 2018.
- [45] Xiao Wang, Tao Sun, Rui Yang, and Bin Luo. Learning target-aware attention for robust tracking with conditional adversarial network. In *30TH British Machine Vision Conference*, 2019.
- [46] Pauline Luc, Camille Couprie, Soumith Chintala, and Jakob Verbeek. Semantic segmentation using adversarial networks. *arXiv preprint arXiv:1611.08408*, 2016.
- [47] Tharindu Fernando, Simon Denman, Sridha Sridharan, and Clinton Fookes. Task specific visual saliency prediction with memory augmented conditional generative adversarial networks. In *2018 IEEE Winter*

- Conference on Applications of Computer Vision*, pages 1539–1548. IEEE, 2018.
- [48] Fang-Yi Chao, Lu Zhang, Wassim Hamidouche, and Olivier Deforges. Salgan360: Visual saliency prediction on 360 degree images with generative adversarial networks. In *2018 IEEE International Conference on Multimedia & Expo Workshops*, pages 01–04. IEEE, 2018.
- [49] Saining Xie and Zhuowen Tu. Holistically-nested edge detection. In *Proceedings of the IEEE international conference on computer vision*, pages 1395–1403, 2015.
- [50] Liang-Chieh Chen, Jonathan T Barron, George Papandreou, Kevin Murphy, and Alan L Yuille. Semantic image segmentation with task-specific edge detection using cnns and a discriminatively trained domain transform. In *Proceedings of the IEEE conference on computer vision and pattern recognition*, pages 4545–4554, 2016.
- [51] Kaiming He, Xiangyu Zhang, Shaoqing Ren, and Jian Sun. Deep residual learning for image recognition. In *Proceedings of the IEEE conference on computer vision and pattern recognition*, pages 770–778, 2016.
- [52] Liang-Chieh Chen, George Papandreou, Iasonas Kokkinos, Kevin Murphy, and Alan L Yuille. Deeplab: Semantic image segmentation with deep convolutional nets, atrous convolution, and fully connected crfs. *IEEE transactions on pattern analysis and machine intelligence*, 40(4):834–848, 2017.
- [53] Jia Deng, Wei Dong, Richard Socher, Li-Jia Li, Kai Li, and Li Fei-Fei. Imagenet: A large-scale hierarchical image database. In *2009 IEEE conference on computer vision and pattern recognition*, pages 248–255. Ieee, 2009.
- [54] Nian Liu, Junwei Han, and Ming-Hsuan Yang. Picanet: Learning pixel-wise contextual attention for saliency detection. In *Proceedings of the IEEE Conference on Computer Vision and Pattern Recognition*, pages 3089–3098, 2018.
- [55] Alex Graves, Navdeep Jaitly, and Abdel-rahman Mohamed. Hybrid speech recognition with deep bidirectional lstm. In *2013 IEEE workshop on automatic speech recognition and understanding*, pages 273–278. IEEE, 2013.
- [56] Pieter-Tjerk De Boer, Dirk P Kroese, Shie Mannor, and Reuven Y Rubinstein. A tutorial on the cross-entropy method. *Annals of operations research*, 134(1):19–67, 2005.
- [57] Jiang-Jiang Liu, Qibin Hou, Ming-Ming Cheng, Jiashi Feng, and Jianmin Jiang. A simple pooling-based design for real-time salient object detection. In *Proceedings of the IEEE Conference on Computer Vision and Pattern Recognition*, pages 3917–3926, 2019.
- [58] Ran Ju, Ling Ge, Wenjing Geng, Tongwei Ren, and Gangshan Wu. Depth saliency based on anisotropic center-surround difference. In *2014 IEEE International Conference on Image Processing*, pages 1115–1119. IEEE, 2014.
- [59] Houwen Peng, Bing Li, Weihua Xiong, Weiming Hu, and Rongrong Ji. Rgbd salient object detection: A benchmark and algorithms. In *European conference on computer vision*, pages 92–109. Springer, 2014.
- [60] Deqing Sun, Stefan Roth, and Michael J Black. Secrets of optical flow estimation and their principles. In *2010 IEEE computer society conference on computer vision and pattern recognition*, pages 2432–2439. IEEE, 2010.
- [61] Ali Borji, Ming-Ming Cheng, Huaizu Jiang, and Jia Li. Salient object detection: A benchmark. *IEEE transactions on image processing*, 24(12):5706–5722, 2015.
- [62] Deng-Ping Fan, Ming-Ming Cheng, Yun Liu, Tao Li, and Ali Borji. Structure-measure: A new way to evaluate foreground maps. In *Proceedings of the IEEE international conference on computer vision*, pages 4548–4557, 2017.
- [63] Radhakrishna Achanta, Sheila Hemami, Francisco Estrada, and Sabine Susstrunk. Frequency-tuned salient region detection. In *2009 IEEE conference on computer vision and pattern recognition*, pages 1597–1604. IEEE, 2009.
- [64] Diederik P Kingma and Jimmy Ba. Adam: A method for stochastic optimization. *arXiv preprint arXiv:1412.6980*, 2014.
- [65] David Feng, Nick Barnes, Shaodi You, and Chris McCarthy. Local background enclosure for rgb-d salient object detection. In *Proceedings of the IEEE Conference on Computer Vision and Pattern Recognition*, pages 2343–2350, 2016.
- [66] Karen Simonyan and Andrew Zisserman. Very deep convolutional networks for large-scale image recognition. *arXiv preprint arXiv:1409.1556*, 2014.
- [67] Wenguan Wang, Qixia Lai, Huazhu Fu, Jianbing Shen, and Haibin Ling. Salient object detection in the deep learning era: An in-depth survey. *arXiv preprint arXiv:1904.09146*, 2019.



**Bo Jiang** received the B.S. degrees in mathematics and applied mathematics and the M.Eng. and Ph.D. degree in computer science from Anhui University of China in 2009, 2012, and 2015, respectively. He is currently an associate professor in computer science at Anhui University. His current research interests include image feature extraction and matching, data representation and learning.



**Zitai Zhou** is currently a Master student in computer science at Anhui University. His current research interests include saliency detection, RGB-D image analysis.



**Xiao Wang** received the B.S. degree in West Anhui University, Luan, China, in 2013. He received the Ph.D. degree in computer science in Anhui University, Hefei, China, in 2019. He is now a postdoc in Pengcheng Laboratory. From 2015 and 2016, he was a visiting student with the School of Data and Computer Science, Sun Yat-sen University, Guangzhou, China. He also have a visiting at UBTECH Sydney Artificial Intelligence Centre, the Faculty of Engineering, the University of Sydney, in 2019. His current research interests mainly about computer vision, machine learning, pattern recognition and deep learning. He serves as a reviewer for a number of journals and conferences such as IEEE TCSVT, TIP, PR, CVPR, ICCV, ECCV and AAAI.



**Jin Tang** received the B.Eng. degree in automation in 1999, and the Ph.D. degree in computer science in 2007 from Anhui University, Hefei, China. Since 2012, he has been a professor at the School of Computer Science and Technology at the Anhui University. His research interests include image processing, pattern recognition and computer vision.



**Bin Luo** received his B.Eng. degree in electronics and M.Eng. degree in computer science from Anhui University of China in 1984 and 1991, respectively. In 2002, he was awarded the Ph.D. degree in Computer Science from the University of York, the United Kingdom. He has published more than 200 papers in journal and refereed conferences. He is a professor at Anhui University of China. At present, he chairs the IEEE Hefei Subsection. He served as a peer reviewer of international academic journals such as IEEE Trans. on PAMI, Pattern Recognition, Pattern Recognition Letters, etc. His current research interests include random graph based pattern recognition, image and graph matching, spectral analysis.